Proceedings of 20th International Congress on Acoustics, ICA 2010

23–27 August 2010, Sydney, Australia

A wave based model to describe the niche effect in sound transmission loss determination of single and double walls

Arne Dijckmans, Gerrit Vermeir

Afdeling Akoestiek en Thermische Fysica - Afdeling Bouwfyscia, K.U.Leuven,
Celestijnenlaan 200 D, B-3001 Heverlee, Belgium

PACS: 43.55.Rg, 43.55.Nd, 43.55.Ti

ABSTRACT

In building acoustical laboratories, the sound transmission loss of structures is typically measured by placing the structure in an aperture between two reverberant rooms. It is known that the location of the specimen in the aperture can affect the results due to the niche - or tunneling - effect. In this paper, a Wave Based Model is used to numerically investigate the tunneling effect in sound transmission loss determination of single and double walls. The field variables (plate displacements and sound pressures) are expanded in terms of structural and acoustic wave functions. The model is validated with experimental results of lightweight single walls. A parametric study for single and double glazing shows that the position of the wall in the opening can significantly influence sound transmission loss below coincidence. As for single walls, the sound transmission loss of double walls is minimal when placed in the center of the niche opening and maximal for the edge positions. The difference, however, is greater for double walls in the mid-frequency range, where sound transmission is highly dependent on the angle of incidence.

INTRODUCTION

An important issue in sound insulation measurements has been the reproducibility, consistency and accuracy. Significant differences are observed in sound transmission loss (STL) when measured in different laboratories [1, 2, 3]. Round-robin tests have shown that room design is important [1], which eventually led to standard design rules for building acoustical laboratories [4]. In the low-frequency range, the modal behaviour of the reverberant rooms and the structure under investigation, which depends on room dimensions, aperture dimensions and aperture placement, can significantly influence the measured STL [2]. The fixing of panels and windows may also give important differences, as the total loss factor of the structure is changed [3].

Several experimental studies have shown the importance of the niche effect [1, 5, 6, 7]. In a study on the influence of the design of transmission rooms on the sound transmission of glass, the position of the sample in the niche had the most important influence on STL [7]. Also the size and depth of the aperture influences STL [1, 3]. All experimental results show that the niche effect is clearly visible below coincidence, while the position of the sample in the niche has no significant influence above the coincidence frequency. Moreover, lowest STL values are obtained when the panel is located at the center of the niche. When the panel is located at one of the edges of the aperture, highest STL values are measured. Most experiments were carried out with lightweight single walls. Cops *et al.* [7] also did measurements on double glazing. The same tendencies were visible as for single glazing measurements.

When analytically calculating sound transmission loss, the niche effect is often incorporated by using a maximum angle of incidence. In this way, the shielding of the test element surface from sound waves that impinge upon the element at near-grazing angles of incidence is taken into account [8]. This gives reasonable results when applied to single-layered structures. The method however gives unrealistic results for double-layered partitions, because the sound transmission loss of double walls is highly dependent on the angle of incidence [9]. Only recently, theoretical approaches to study the niche effect have been published. Kim *et al.* [10] calculated transmission loss for a 1D single panel placed in a niche in an infinite baffle. Vinokur [11] tried to give a physical explanation of the niche effect, which he defined as the difference in STL for the center and edge locations of the specimen. The model, approximately valid for frequencies $f < c_{air}/\sqrt{S}$, with c_{air} the speed of sound in air and S the aperture area, indicates that the niche effect does not depend on the specimen parameters but only on the aperture dimensions and frequency.

This paper gives a theoretical approach of the niche effect for single and double walls. The two-dimensional structure is placed in a niche between two 3D rectangular reverberant rooms. The direct sound transmission loss is calculated by use of a wave based method. The model takes into account the full coupling between the room modes, the niche modes, the cavity modes and the bending wave modes of the plates. This is important, as the amount of coupling between niche, cavity and plate modes determines sound transmission.

WAVE BASED MODEL

The Wave Based Method (WBM) is a Trefftz-based deterministic prediction method for the steady-state dynamic analysis of coupled vibro-acoustic systems. A general description of the method can be found in [12]. In this method, the steady-state dynamic variables (sound pressures and plate displacements) are expressed in terms of a set of wave functions which are solutions of the homogeneous parts of the governing dynamic equations, completed with a particular solution function of the

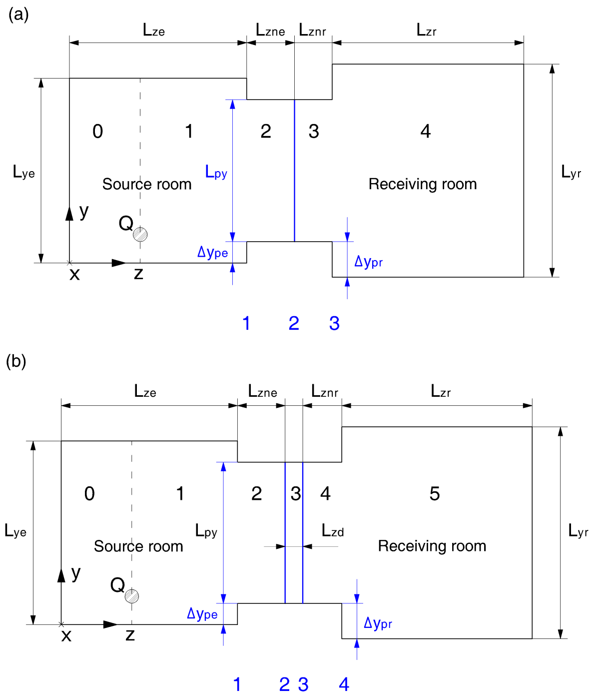

Figure 1: Geometry of the considered problem: STL of structure placed in a niche between two reverberant rooms: (a) single wall (b) double wall.

inhomogeneous equation. Since the functions are exact solutions of the governing equations, the contribution of a certain function in a set is merely determined by the (vibro-)acoustic boundary conditions. As only a finite number of functions can be considered, the boundary conditions can only be satisfied approximately. The wave based model described in this section is based on the model presented in [13].

Problem definition

The geometry of the considered problem is shown in Figure 1. A rectangular single or double wall with dimensions L_{px} and L_{py} is placed in a niche between two rectangular 3D rooms. Source and receiving room have dimensions $L_{xe} \times L_{ye} \times L_{ze}$ and $L_{xr} \times L_{yr} \times L_{zr}$ respectively. The niche has a depth L_{zne} at emitting side and a depth L_{znr} at receiving side. In source and receiving room, uniform damping is taken into account as function of the reverberation time T. To calculate the sound transmission loss, a harmonic volume point source is placed in the source room at position (x_s, y_s, z_s).

Rooms and air cavities

The source room is divided into two parts by a plane through the point source, parallel to the back wall. For the single wall problem, one gets 5 subdomains (2 in the source room, niche at emitting side, niche at receiving side and receiving room). In the case of a double wall, the air cavity is considered as an extra subdomain. The steady-state acoustical pressure in each subdomain $\underline{p}_{a,i}$ (single wall: $i = 0 \ldots 4$, double wall: $i = 0 \ldots 5$) is governed by the homogeneous Helmholtz equation,

$$\nabla^2 \underline{p}_{a,i}(x,y,z) + k_a^2 \underline{p}_{a,i}(x,y,z) = 0. \tag{1}$$

$k_a = \frac{\omega}{c_{air}}$ is the acoustic wavenumber in air, with ω the circular frequency and c_{air} the speed of sound in air. In source and receiving room, uniform damping is introduced by making the acoustic wavenumber complex:

$$\underline{k}_a = k_a \left(1 - j\,\frac{1}{2}\,\frac{fT}{2.2}\right), \tag{2}$$

where T is the reverberation time of the room. f is the frequency, $j = \sqrt{-1}$.

Thin plates

For acoustically thin plates, the transverse displacement $\underline{w}_i$ of the plate at position $z = z_{pi}$ (single wall: $i = 2$, double wall: $i = 2,3$) fulfils Kirchhoff's thin plate bending wave equation,

$$\left(\nabla^4 - \underline{k}_{B,i}^4\right) \underline{w}_i(x,y) = \frac{\underline{p}_{a,i}(x,y,z_{pi}) - \underline{p}_{a,i+1}(x,y,z_{pi})}{\underline{B}_i'}, \tag{3}$$

where the bending wave number $\underline{k}_{B,i}$ and the plate bending stiffness $\underline{B}_i'$ are defined as

$$\underline{k}_{B,i} = \sqrt[4]{\frac{m_i''\omega^2}{\underline{B}_i'}} \quad \text{and} \quad \underline{B}_i' = \frac{E_i h_i^3 (1 + j\eta_i)}{12(1 - \nu_i^2)}, \tag{4}$$

with $m_i'' = \rho_i h_i$ the surface mass density of plate i, h_i the plate's thickness. The material of plate i has a density ρ_i, a Young-modulus E_i, a loss factor η_i and a Poisson coefficient ν_i.

Field variable expansion

The acoustic pressures are approximated in terms of the following acoustic wave function expansion,

$$\underline{p}_{a,i}(x',y',z') = \sum_m \sum_n \left(e^{-j\underline{k}_{zimn}z'} \underline{P}_{imn} + e^{j\underline{k}_{zimn}z'} \underline{Q}_{imn}\right) \times \varphi_{imn}(x',y'), \tag{5}$$

where

$$\varphi_{imn}(x',y') = \cos\left(\frac{m\pi}{L_{xi}}x'\right) \cos\left(\frac{n\pi}{L_{yi}}y'\right) \tag{6}$$

and

$$\underline{k}_{zimn} = \sqrt{\underline{k}_{a,i}^2 - \left(\frac{m\pi}{L_{xi}}\right)^2 - \left(\frac{n\pi}{L_{yi}}\right)^2}. \tag{7}$$

L_{xi} and L_{yi} are the cross-sectional dimensions of the room, niche or cavity. The local coordinate systems (x',y',z') are defined as follows: $(x',y',z') = (x,y,z)$ for source room $(i = 0,1)$, $(x',y',z') = (x - \Delta x_{pe}, y - \Delta y_{pe}, z - z_{p(i-1)})$ for the niches and cavity (single wall: $i = 2,3$, double wall: $i = 2 \ldots 4$), $(x',y',z') = (x - \Delta x_{pe} + \Delta x_{pr}, y - \Delta y_{pe} + \Delta y_{pr}, z - z_{p(i-1)})$ for the receiving room (single wall: $i = 4$, double wall: $i = 5$). The wave functions are exact solutions of the homogeneous Helmholtz equation (1).

Eq. (5) leads to following wave function expansion for the particle displacement in the z-direction,

$$\underline{w}_{a,i}(x',y',z') = -\frac{j}{\omega^2 \rho_{air}} \sum_m \sum_n \left(e^{-j\underline{k}_{zimn}z'} \underline{P}_{imn} - e^{j\underline{k}_{zimn}z'} \underline{Q}_{imn}\right) \times \underline{k}_{zimn} \varphi_{imn}(x',y'), \tag{8}$$

with ρ_{air} the density of air.

Following wave function expansion is used for the transverse displacement of the plates:

$$\underline{w}_i(x,y) = \sum_p \sum_q \underline{A}_{ipq} \varphi_{pimn}(x,y). \tag{9}$$

Assuming simply supported plates, following expansion functions are used:

$$\varphi_{pimn}(x,y) = \sin\left(\frac{p\pi}{L_{px}}(x - \Delta x_{pe})\right) \sin\left(\frac{q\pi}{L_{py}}(y - \Delta y_{pe})\right). \tag{10}$$

The proposed pressure expansions satisfy a priori the rigid side wall boundary conditions. The plate displacement expansions satisfy a priori the simply supported boundary conditions.

Continuity and boundary conditions

In the source room, a rigid back wall is assumed,

$$\underline{w}_{a,0}\Big|_{z'=0} = 0. \tag{11}$$

In the receiving room (single wall: $i = 4$, double wall: $i = 5$), the rigid back wall assumption gives following boundary condition:

$$\underline{w}_{a,i}\Big|_{z'=L_{zr}} = 0. \tag{12}$$

At the source plane $z = z_s$, continuity of pressure and particle velocity is imposed,

$$\underline{p}_{a,0}\Big|_{z'=z_s} = \underline{p}_{a,1}\Big|_{z'=z_s}, \tag{13}$$

$$j\omega\underline{w}_{a,0}\Big|_{z'=z_s} + \delta(x'-x_s, y'-y_s) = j\omega\underline{w}_{a,1}\Big|_{z'=z_s}. \tag{14}$$

At the interface between the niche and the source, continuity of pressure and normal particle displacement is imposed,

$$\underline{p}_{a,1}\Big|_{z'=L_{ze}} = \underline{p}_{a,2}\Big|_{z'=0}, \tag{15}$$

$$\underline{w}_{a,1}\Big|_{z'=L_{ze}} = \underline{w}_{a,2}\Big|_{z'=0}. \tag{16}$$

Similar continuity conditions have to be fulfilled at the niche-receiving room interface (single wall: $i = 3$, double wall: $i = 4$),

$$\underline{p}_{a,i}\Big|_{z'=L_{znr}} = \underline{p}_{a,i+1}\Big|_{z'=0}, \tag{17}$$

$$\underline{w}_{a,i}\Big|_{z'=L_{znr}} = \underline{w}_{a,i+1}\Big|_{z'=0}. \tag{18}$$

At the plates surfaces, continuity of transverse displacement is imposed (single wall: $i = 2$, double wall: $i = 2, 3$),

$$\underline{w}_i = \underline{w}_{a,i}\Big|_{z'=L_{zi}}, \tag{19}$$

$$\underline{w}_i = \underline{w}_{a,i+1}\Big|_{z'=0}. \tag{20}$$

Method of solution

The participation factors in the expansions (5) and (9) are determined by the boundary and continuity conditions (11)-(20) and the equations of motion (3) of each plate. The boundary and continuity condition errors are forced to zero in an integral sense through the application of a Galerkin-like weighted residual formulation [12, 13].

For the interface conditions (15)-(18), an auxiliary variable $\underline{w_i}$ is introduced. The particle displacement at the interfaces is expanded in a series of the form (9)-(10), similar to the plate displacement expansions. Consequently, one gets an equivalent problem with 3 (or 4) plates, separated by air cavities, for a single (or double) wall placed in a niche. The particle displacement continuity conditions (16) and (18) are replaced by 4 equivalent continuity conditions of the forms (19)-(20). The pressure continuity conditions (15) and (17) can be interpreted as an equivalent equation of motion of the form (3), with the left hand side put to zero.

Because of the simple rectangular geometry, the factors $\underline{P}_{imn}$ and $\underline{Q}_{imn}$ can be eliminated analytically in function of the primary unknowns $\underline{A}_{ipq}$, by use of the weighted residual formulations of the boundary and interface conditions. The (equivalent) equations of motion of the plates then result in a symmetric matrix of equations in the unknowns $\underline{A}_{ipq}$.

Calculation of STL

The sound transmission loss (STL) is determined by the measurement formula,

$$STL = L_{pe} - L_{pr} + 10\log\frac{S}{A_r}. \tag{21}$$

The sound pressure levels in emitting and receiving room L_{pe} and L_{pr} are calculated by analytical integration of the acoustic pressure over the respective room volumes. S is the surface area of the element and $A_r = \frac{0.16V_r}{T_r}$ the absorption area of the receiving room, with V_r the volume and T_r the reverberation time.

STL is calculated at 81 frequencies per third octave band. The average STL in each frequency band is calculated from the summated sound pressure levels $L_{p,1/3\ octave}$,

$$L_{p,1/3\ octave} = 10\log\left(\sum_{i=1}^{81} 10^{L_{p,i}/10}\right). \tag{22}$$

NUMERICAL AND EXPERIMENTAL VALIDATION

Continuity and convergence analysis

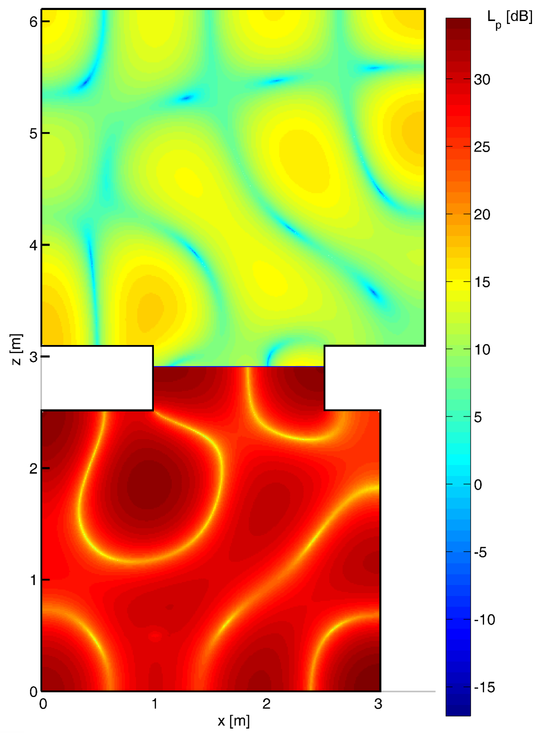

Figure 2: 9.5 mm glass in niche (2D): pressure at 200 Hz. Source position (x_s,z_s) = (1.0 m, 0.5 m).

In order to validate the wave based model, a two-dimensional case is examined. The geometry can be seen in Figure 2. In the source room, with dimensions 3.0 m × 2.5 m, a point source is placed at position (x_s,z_s) = (1.0 m, 0.5 m). The receiving room has dimensions 3.5 m × 3.0 m. A glass pane with thickness 9.5 mm and length 1.5 m is placed at a position 2:1 within a niche with depth 0.6 m. The glass has a density ρ = 2420 kg/m^3, an elasticity modulus E = 62000 MPa, a Poisson coefficient ν = 0.23 and a total loss factor η = 0.025. Figure 2 shows the pressure predictions at 200 Hz, obtained with a wave based model, consisting of 300 acoustic wave functions in each (sub)room and niche, and 300 structural wave functions for each (auxiliary)

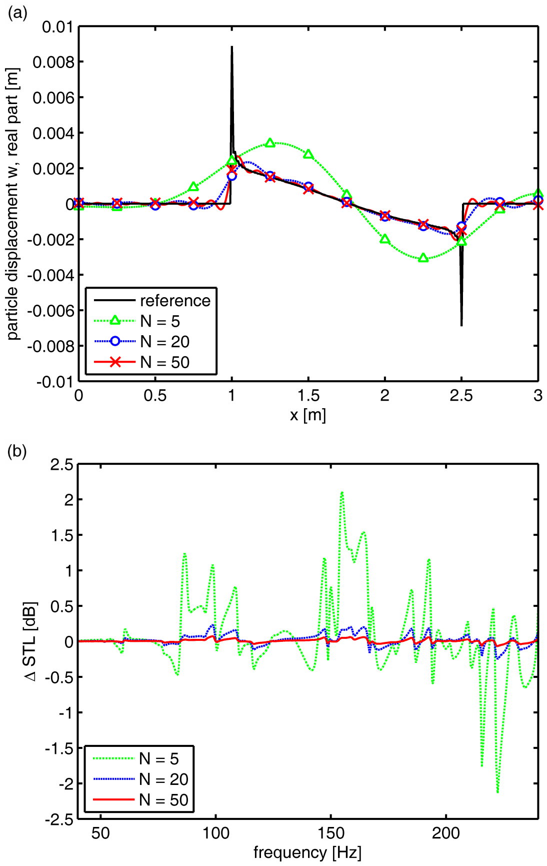

Figure 3: 9.5 mm glass in niche (2D): convergence of (a) particle displacement at source room - niche interface at 200 Hz (b) STL. Δ STL is the difference in STL with the reference solution (N = 300). N is the number of room-, plate- and nichemodes used in the expansions.

plate displacement. The figure illustrates that the pressure continuity conditions at the room-niche interfaces are accurately represented. The fact that the pressure contour lines are perpendicular to the rigid walls, indicates that the boundary conditions are also accurately represented.

The most critical approximation error is the continuity of normal particle displacement at the various interfaces (source plane, source room - niche, niche - receiving room). At these interfaces there is a discontinuity in particle displacement. For example at $z = 2.5$ m, $\underline{w} = 0$ at the rigid wall of the source room, whereas at the niche interface $\underline{w} \neq 0$. To accurately describe the particle displacement, one needs enough expansion functions, see Figure 3(a). If one increases the number of functions, the approximation error reduces, so convergence to the right solution is achieved. Overall values like room-averaged pressure levels and STL converge faster to the exact solution (see Figure 3(b)). Therefore, accurate STL values (error less than 0.1 dB) can be obtained with a reasonable number of expansion functions. Convergence is guaranteed if (1) a minimal number of expansion functions, depending on frequency, is used and (2) the number of auxiliary plate modes (which gives the number of continuity condition equations imposed) is lower or equal to the number of room and niche modes.

Single fiberboard plate

The sound transmission loss of a single fiberboard plate was measured with the pressure method according to ISO 140-3 in the transmission chambers of the Laboratory of Acoustics at the K.U.Leuven. Each transmission chamber has a volume of 87 m^3. The fiberboard plate has dimensions 1.25 m × 1.50 m, see Figure 4. Detailed sections of the measurement aperture are shown in Figure 5. The staggered niche has been changed to a flat one at both sides of the panel, creating a tunnel with dimensions 1.25 m × 1.50 m and a depth of 0.40 m. The fiberboard plate is placed in the tunnel, resulting in niche-depths L_{zne} = 0.15 m at emitting side and L_{znr} = 0.25 m at receiving side. At the receiving side, the outer niche was also partly covered with a plasterboard construction. The results are compared with a wave based model with and without niche. In the wave based model with niche, the outer niche (with dimensions 1.80 m × 1.90 m) is neglected as a first approximation. In the simulations, a plate density ρ = 675 kg/m^3, an elasticity modulus E = 3500 MPa and a Poisson coefficient ν = 0.48 are used for the fiberboard. For the total loss factor of the plate and the reverberation times of emitting and receiving room, measured values are used.

Figure 4: Measurement setup: fiberboard 9.5 mm with dimensions 1.25 m × 1.50 m.

Figure 6 shows the measurement and simulation results of the sound transmission loss in 1/48 octave bands. Three frequency regions can be recognized. In the low frequency range, till approximately 250 Hz in this case, the sound transmission is dominated by the modal behaviour of rooms and structure. The dynamic range is very large. From 250 Hz till 1600 Hz, sound transmission is determined by the mass of the structure. Here, non-resonant transmission is dominant, resulting in the well-known mass-law behaviour. Above 1600 Hz, the coincidence dip, determined by the bending stiffness of the plate, is clearly visible.

The wave based model without niche gives reasonable predictions, see Figure 6(a). However, there are some slight discrepancies. In the low frequency range, STL is overestimated at the resonance dips, resulting in a global overestimation in third octave bands. In the mid-frequency range, the predicted STL is very smooth, whereas the measurement results shows dips and peaks in a range of 8 dB. Thirdly, the measured coincidence dip is broader in comparison with WBM results.

Figure 6(b) shows that the niche-effect can largely explain these differences. The depth of the resonance dips is better predicted in the low frequency range. The niche can also explain the dips

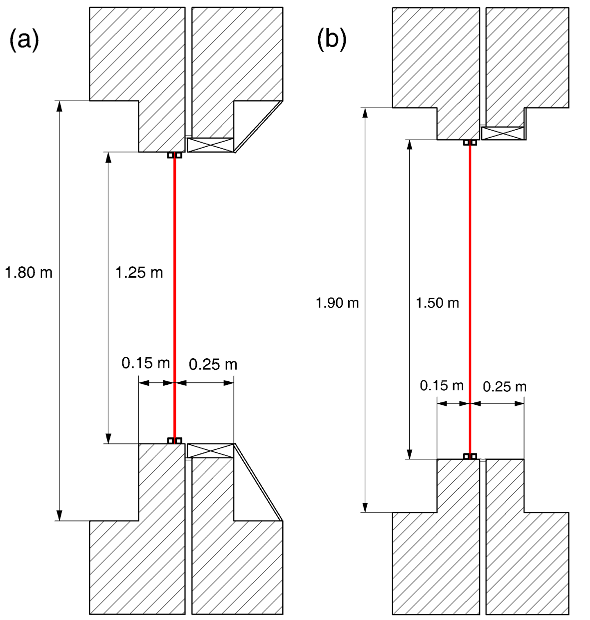

Figure 5: Measurement aperture: (a) horizontal section (b) vertical section.

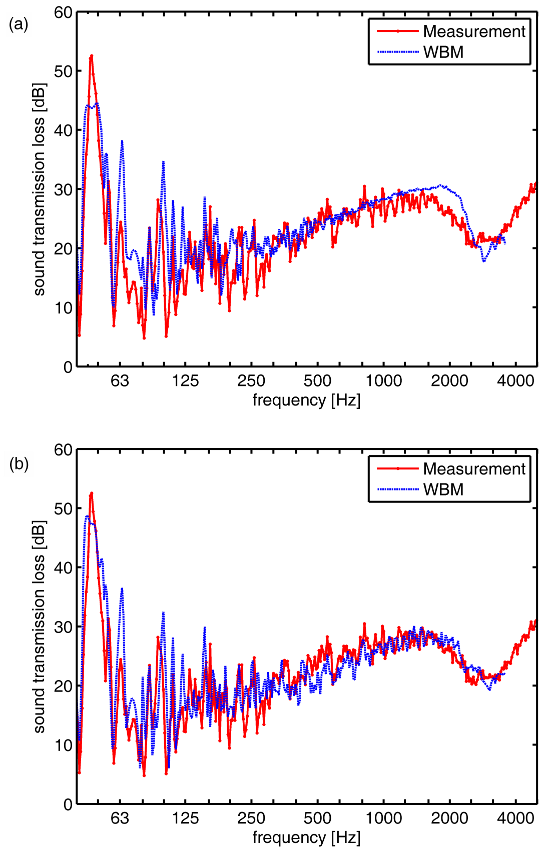

Figure 6: STL fiberboard 9.5 mm: measurement and (a) WBM simulation without niche (b) WBM simulation with niche.

and peaks in the mid-frequency range and the broadening of the coincidence dip. Orthotropic properties of the fiberboard can be another explanation of the broader coincidence dip.

Laminated glass panel

Cops *et al.* [3] measured the sound transmission loss of a laminated glass panel in the transmission chambers of the Laboratory of Acoustics at the K.U.Leuven. The laminated glass panel had dimensions 1.60 m × 1.30 m and 4 mm glass - 0.76 mm buthyl - 4 mm glass thickness. The influence of the placement of the glass in the measurement opening was investigated. The panel was placed in an extreme position (niche depth 0.00 m and 0.70 m) and nearly centrally placed (niche depth 0.30 m and 0.40 m). The measurement results are shown in Figure 7. The two measurement setups are also simulated with the wave based model. The laminated glass panel is simulated as a single glazing with a thickness of 8 mm, a density ρ = 2500 kg/m^3, an equivalent elasticity modulus E_{eq} = 52 000 MPa and a total loss factor η = 0.10. In the model for the extreme placement, niche depths L_{zne} = 0.05 m and L_{znr} = 0.65 m are used. This is more realistic and gives better agreement with measurement results.

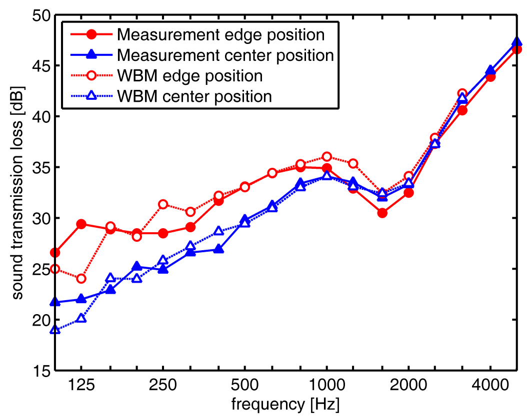

Source: [3]

Figure 7: STL laminated glass 4.4 mm, dimensions 1.60 m × 1.30 m: measurement and WBM predictions for edge location (L_{zne} = 0 m, L_{znr} = 0.70 m) and center location (L_{zne} = 0.30 m, L_{znr} = 0.40 m).

The agreement between the measured and predicted STL values is good, especially for the nearly central position of the panel (see Figure 7). The wave based model is able to predict the influence of the position of the panel in the niche. Below the coincidence frequency, the significant difference between edge and central placement can be seen in both measurement and simulations. Around coincidence, the wave based model overestimates STL for the edge position. A possible explanation can be the overestimation of the total loss factor for this configuration.

PARAMETRIC STUDY

Niche effect for single and double glazing

In the following sections, the 3D wave based model is applied to a single glazing (thickness 9.5 mm) and a double glazing (9.5/12/9.5 mm) with dimensions 2.4 m × 2.4 m. The material properties used are the same as those used for the glass in the continuity and convergence analysis. The glazing is placed inside a niche with depth 0.6 m at three locations: the edge position (L_{zne},L_{znr}) = (0 m, 0.6 m), the normal position (0.2 m, 0.4 m) and the center position (0.3 m, 0.3 m). The prediction results are given in Figure 8. As a reference, the STL calculated

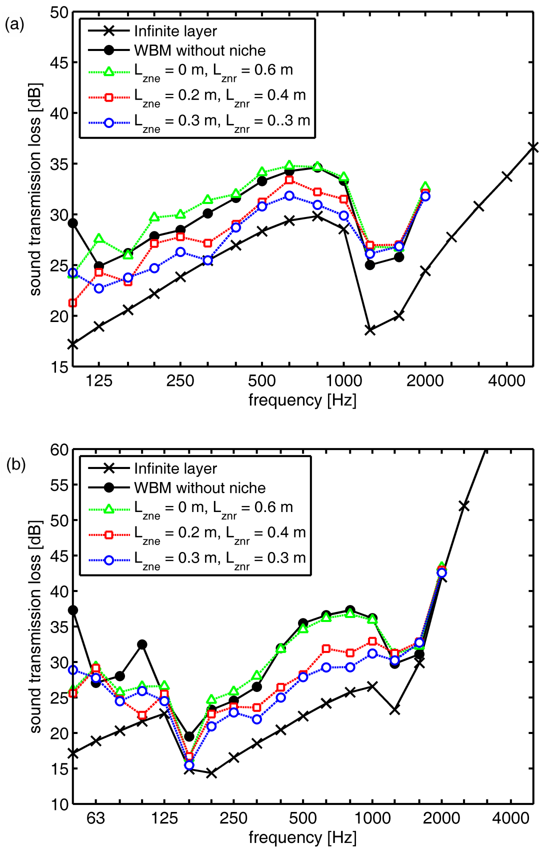

Figure 8: Comparison of STL with and without niche: (a) single glazing 9.5 mm (b) double glazing 9.5/12/9.5 mm.

for the same source and receiving room without niche is shown. The diffuse transmission loss for infinite layers, calculated with a transfer matrix approach, is also given as a comparison.

The third octave prediction results for single glazing (see Figure 8(a)) are similar to the results reported in [10] by Kim *et al*. The niche effect is most obvious below the coincidence frequency around 1250 Hz. Lowest STL values are obtained for the center position. The edge position gives higher values compared to the WBM reference case without niche. This is in contrast with the model of *Kim et al.*, where STL was always lower in the case with niche. The STL is hardly affected by the existence of a niche above the coincidence. The niche effect results in a less pronounced, but broader coincidence dip.

The results for double glazing (see Figure 8(b)) exhibit the same tendencies. At the mass-spring-mass resonance frequency around 160 Hz, the dip is more pronounced in the case with niche, also for the edge position. This phenomenon was also seen in measurements on double glazing done by Yoshimura [8]. In the mid-frequency range, the niche effect reduces STL, except for the edge position. The dip around the coincidence of the glass panes is broadened.

Figure 9 shows the difference between the STL for edge and center position, both for the single and double glazing. It can be seen that in the low frequency range, this difference is approximately independent of the specimen type, as predicted in [11] for frequencies $f < c_{air}/\sqrt{S} = 143$ Hz. The niche effect is negligible around and above the coincidence dips of the glass panels at 1250-1600 Hz. In the mid-frequency range, the double glazing differences are 3 to 4 dB larger compared to single glazing results. This can be expected, as STL of the double wall

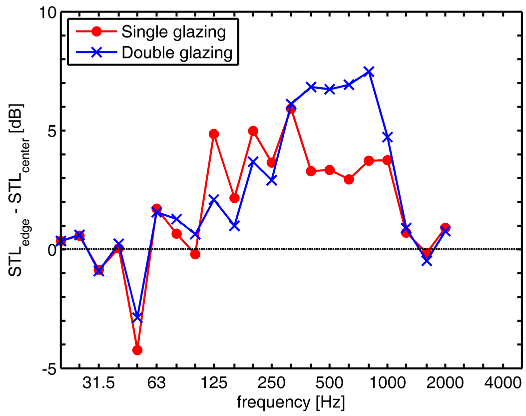

Figure 9: The niche effect for single and double glazing (aperture dimensions 2.4 m × 2.4 m, depth 0.6 m).

is highly dependent on the angle of incidence in this frequency range. Around the mass-spring-mass resonance dip of the double wall, the difference is small, as both the edge and center position decrease STL.

Influence of panel location in the niche

The influence of the panel location in the niche is investigated in this section. The same single and double glazing are placed in a niche with depth $L_{zn} = 0.6$ m at various positions. Figure 10 shows the STL difference between the cases with and without a niche. The changes in STL are shown as a function of normalized panel location, L_{zne}/L_{zn}, for a couple of third octave band values.

For the single glazing (see Figure 10(a)), typical behaviour as reported in literature is found below coincidence. STL is minimal for central location in the niche and maximum for both edge locations. Equal volumes of niches at both sides of the transmitting panel increase the transmission of energy through the panel, especially at its eigenfrequencies, due to the strong coupling of the equal niches on both sides [3]. This strong coupling cannot occur for the edge positions. The coupling can be decreased by the introduction of a staggered niche instead of a flat niche [7]. The artificial modification of the measurement opening by placing a diametrically reflecting plate in the opening has also shown the negative influence of this coupling between the two niches on STL [3].

At the coincidence dip (1250-1600 Hz), the niche improves STL slightly (1-2 dB), almost independent of the panel location. In the low frequency range, for example at 100 Hz, STL is determined by the modal behaviour of rooms, niches and plate. The number of modes and the amount of coupling between the various modes influences sound transmission. Therefore, large differences can occur, but no general behaviour can be indicated.

The results for double glazing (see Figure 10(b)) show the same trends. This confirms the conclusion of Vinokur [11] that to a reasonable approximation, the niche effect does not depend on the specimen parameters but depends on on the aperture dimensions and frequency. However, it can be seen that the niche effects are more pronounced for the double glazing.

Influence of niche depth

The influence of tunnel depth on the niche effect is investigated in detail by increasing the depth from 0 to 1 m. Figure 11 shows

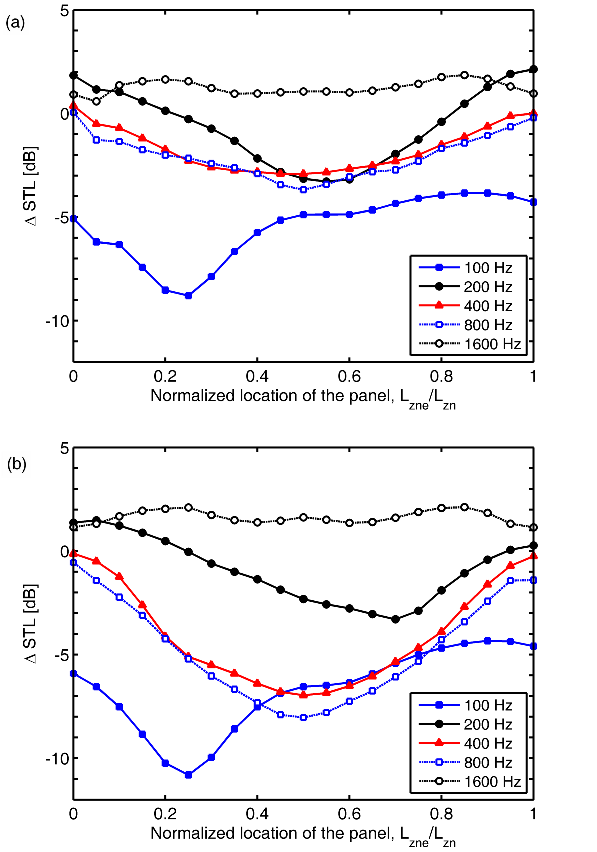

Figure 10: Δ STL variations with panel location in niche with depth L_{zn} = 0.6 m: (a) single glazing 9.5 mm (b) double glazing 9.5/12/9.5 mm.

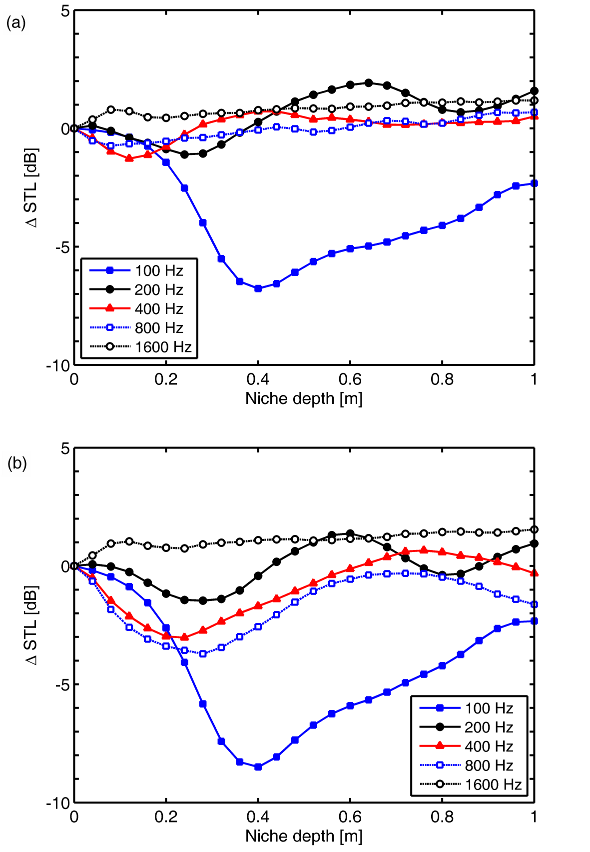

Figure 11: Δ STL variations with niche depth when panel is located at the edge of the niche: (a) single glazing 9.5 mm (b) double glazing 9.5/12/9.5 mm.

Δ STL when the single or double glazing is placed at the source room edge of the niche. For the single glazing, variation of niche depth has limited influence (± 2 dB) on STL. Only in the low-frequency range, larger variations are visible. The influence of niche depth is larger for double glazing results, variations between -4 dB and +2 dB are visible. When the panels are located in the center of the tunnel, the niche effect is more pronounced (see Figure 12). For small niche depths (compared to the wavelength), generally it can be seen that the reduction in STL below coincidence by the niche, increases with increasing niche depth. When the depth is further increased, STL remains more or less the same or is even improved again. Two opposing effects of deeper niches can explain these results [8]. For niche depths $< \lambda/2$, the niche can be modeled as if the plate lies in the plane of the baffle. With niche depths $\geq \lambda/2$, the niche forms a baffle perpendicular to the plate perimeter, doubling the radiation efficiency of the plate modes below coincidence. As a result, resonant transmission is increased with increasing niche depth. On the other hand, non-resonant transmission is decreased for deeper niches due to the shielding of near-grazing angles by the niche.

CONCLUSIONS

In this paper, a wave based model has been developed to investigate the niche effect on sound transmission loss determination. Sound transmission between rooms is dependent on the coupling between acoustic and structural modes. Therefore, the dimensions of the rooms, the position and depth of the aperture and the position of the structure in the niche can influence the measured STL.

When the structure is placed inside a niche, STL values are generally decreased below coincidence, compared to STL values without niche. This can be explained by the strong coupling between the modes at both sides of the tunnel and the interaction with the structural modes, especially for a central placement. For edge positions, this coupling cannot occur. Therefore, predicted STL is highest for both edge positions.

Around and above the coincidence frequency, the niche effect is negligible. The position of the plate in the niche and the niche depth has no influence. Globally, the coincidence dip is broader and less pronounced when a plate is placed in a niche.

In the low frequency range, where modal density is low, the niche effect is largely depending on the specific situation. No general behaviour can be indicated.

The predicted values for a single wall are in agreement with previous measurements and theory. The same tendencies are visible for double walls. However, the effect of the niche on STL of a double wall is larger. Differences in third octave band STL values between edge and central positions tend to be 3 to 4 dB higher than for the single wall in the mid-frequency range. This can be expected, as sound transmission of the double wall is highly dependent on angle of incidence in this frequency range. The mass-spring-mass resonance dip is more pronounced in comparison with the case without a niche.

ACKNOWLEDGEMENTS

Arne Dijckmans is a Doctoral Fellow of the Research Foundation - Flanders (FWO - Vlaanderen).

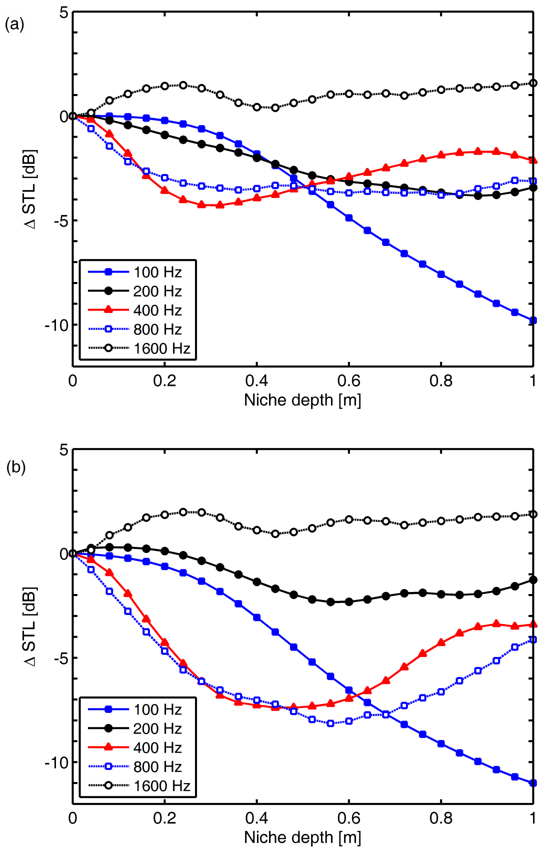

Figure 12: Δ STL variations with niche depth when panel is located at the center of the niche: (a) single glazing 9.5 mm (b) double glazing 9.5/12/9.5 mm.

REFERENCES

[1] T. Kihlman and A. C. Nilsson. “The effect of some laboratory design and mounting conditions on reduction index measurements”. *J. Sound Vib.* 24.3 (1972), pp. 349–364.

[2] A. Osipov, P. Mees, and G. Vermeir. “Low-frequency airborne sound transmission through single partitions in buildings”. *Appl. Acoust.* 52.3/4 (1997), pp. 273–288.

[3] A. Cops, M. Minten, and H. Myncke. “Influence of the design of transmission rooms on the sound transmission loss of glass - Intensity versus conventional method”. *Noise Control Eng. J.* 28.3 (1987), pp. 121–129.

[4] *ISO 140-1:1997 Acoustics - Measurement of sound insulation in buildings and of building elements - Part 1: Requirements for laboratory test facilities with suppressed flanking transmission.*

[5] R. W. Guy and P. Sauer. “The influence of sills and reveals on sound transmission loss”. *Appl. Acoust.* 17.6 (1984), pp. 453–476.

[6] R. E. Halliwell and A. C. C. Warnock. “Sound transmission loss: Comparison of conventional techniques with sound intensity techniques”. *J. Acoust. Soc. Am.* 77.6 (1985), pp. 2094–2103.

[7] A. Cops and D. Soubrier. “Sound transmission loss of glass and windows in laboratories with different room design”. *Appl. Acoust.* 25.4 (1988), pp. 269–280.

[8] C. Hopkins. “Sound insulation”. Elsevier Ltd., Oxford, UK, 2007. Chap. 3, pp. 253–258.

[9] S. Kurra and D. Arditi. “Determination of sound transmission loss of multilayered elements part 1: Predicted and measured results”. *Acta Acust. united Ac.* 87.5 (2001), pp. 582–591.

[10] B. K. Kim et al. “Tunneling effect in sound transmission loss determination: Theoretical approach”. *J. Acoust. Soc. Am.* 115.5 (2004), pp. 2100–2109.

[11] R. Vinokur. “Mechanism and calculation of the niche effect in airborne sound transmission”. *J. Acoust. Soc. Am.* 119.4 (2006), pp. 2211–2219.

[12] W. Desmet. “A wave based prediction technique for coupled vibro-acoustic analysis”. PhD thesis. Katholieke Universiteit Leuven, Departement Werktuigkunde, 1998.

[13] A. Dijckmans and G. Vermeir. “Application of the wave based prediction technique to building acoustical problems”. *Proc. of ISMA2010, Leuven*. 2010.